Effects of the characteristics of a force-driven bulkhead on the structural acoustics of an elastic cylinder

Langdon C. Heath[1], Naveendra Fernando[1], Hongmei Sun[1], David Matthews[2,1]

and Jie Pan[1]

[1]School of Mechanical & Chemical Engineering, The University of Western Australia, Australia
[2]Defence Science & Technology Group, HMAS Stirling, GPO Box 2188, Rockingham DC WA 6967, Australia

ABSTRACT

To study the structural acoustics of propeller-excited marine vessels, the hull and bulkhead, against which the thrust bearing is mounted, are often modelled as a circular cylinder and a cross-section plate. This paper concerns the effects of the characteristics of the cross-section plate on the vibration and radiated sound from the cylinder. The critical aspect is the coupling between the plate and cylinder, as this affects the input power of the excitation force at the plate and energy transfer from the plate to the cylinder and eventually to the radiated sound. The study compares the input mobility, averaged vibration response of the cylinder, and the radiated sound power with respect to the driving force for full-plate and half-plate configurations. Conditions associated with large sound power radiation from the cylinder are assessed through detailed measurement of the distributed sound intensity and vibration on the surface of the cylinder. The results demonstrate the drastic differences in the radiated sound power when different cross-section plates are used, and indicate the importance of coupling between the hull and bulkhead structure for controlling the radiated sound power from the propeller-driven hull–bulkhead structure.

1. INTRODUCTION

The ability to control sound radiation from surface and submerged marine vessels is a key area of concern for ship operation, the ocean noise environment (Tyack, 2008), and underwater measurement. One of the major sources of sound radiation from a marine vessel is the vibration of the hull structure (Caresta & Kessissoglou, 2010). This excitation is primarily due to the fluctuating force generated during propeller operation (Leader *et al*., 2013), transmitted to the hull structure via the propeller shaft and thrust-bearing bulkhead. In particular, low-frequency noise radiation from the hull can propagate large distances without significant attenuation. Therefore, a clear understanding of the structural acoustics of a propeller-driven structure is crucial for effectively controlling the radiated sound from marine vessels.

Although the general structural acoustics of hull structures has been studied extensively (Soedel, 2004, Fahy, 1987, Leissa, 1973, Caresta & Kessissoglou, 2009, Gangemi & Kanapathipillai, 2014, Merz *et al*., 2006), little research has focused on the effects of the characteristics of the thrust-bearing bulkhead on the structural acoustics. In this paper, this effect is illustrated by experimentally comparing two cylinder/plate models, where the only difference between the models is that the cross-section plate is either a full or half plate. Experimental evidence is presented to show that variation in the cross-section plate will cause a significant change in the input mobility at the driving location of the plate, in the averaged vibration level of the cylinder, and the radiated sound power from the cylinder.

2. DESCRIPTION OF THE EXPERIMENTAL SET-UP

Figure 1 shows the experimental set-up used for this work. It consists of a circular cylinder of length 1.408 m, outer diameter 209.9 mm, and thickness 4 mm. The ends of the cylinder are connected with 17-mm-thick outer flanges with external diameter 335 mm. Two 14 mm thick plates with external diameter 335 mm are bolted to both ends of the cylinder with the top end containing a 16 mm diameter hole, allowing access to the inside of the cylinder. The internal cross-section plate is bolted to the cylinder (at twelve locations an equal distance apart) through an internally welded annulus. One plate has an internal half-circular section cut out and the other is complete. Both plates have diameter 199.5 mm and thickness 3 mm and are located at 250 mm from the top-end of the cylinder. The plates will be referred to as the half plate and the full plate, respectively. All components are made from steel.

The entire structure was suspended vertically in air with rubber springs attached to the cylinder's flange. The first two natural frequencies of the rubber springs are 20 Hz and 35 Hz. A B&K 4810 mini-shaker was attached to the centre of the internal plate using a magnetic stud. A B&K 8001 impedance head was inserted between the plate and shaker. The connection between the shaker and the impedance head was a thin steel stinger with exposed length 25 mm and diameter 2 mm. The shaker force output was uncalibrated and had a force sensitivity of 3.16 V/N and acceleration sensitivity of 100 mV/m/s^2. Effects of mass loading on plate vibration were minimised using a pulley system to balance the static weight of the shaker. Data acquisition was completed using a B&K Pulse system with a frequency resolution of 1 Hz.

The frequency response function (FRF) of the structure's vibration was measured below 1600 Hz using white noise excitation. This data was recorded from eight PCB 352C67 accelerometers, with sensitivities of approximately 10 mV/m/s^2. The location of each accelerometer is shown in Figure 2B. The spatially averaged acceleration $< A >$ with respect to the driving force F was used to describe the overall cylinder response:

$$\frac{< A >}{|F|} = \sqrt{\frac{1}{M}\sum_{m=1}^{M}\frac{A_m^2}{F^2}}\,, \tag{1}$$

where M is the number of accelerometers on the cylinder. The input mobility was measured via the outputs of the impedance head:

$$|Y| = \left|\frac{A_F}{\omega F}\right|, \tag{2}$$

where ω is the angular frequency and A_F is the acceleration at the driving location. Two microphones in a sound intensity probe (with a 50-mm spacer, suitable for the 1/3 octave centre frequencies up to 1.25 kHz) were used to record the sound pressure adjacent to the cylinder's surface. This measurement was performed at sixteen accessible locations, evenly distributed around the cylinder, as indicated in Figure 2. The FRFs of the measured pressures (p_1 and p_2, where p_1 is from the microphone closest to the cylinder) were used to determine the narrow-band sound intensity (with respect to the force) at those locations:

$$\frac{I_R}{F^2} = -\frac{1}{2\rho\omega d}\left|\frac{p_1}{F}\right|\left|\frac{p_2}{F}\right|\sin(\theta) \tag{3}$$

where ρ is the mass density of air, d is the distance between the two microphones, p_1 and p_2 are the frequency domain pressure measurements, and θ is the phase angle of the frequency response function given by $\frac{p_2}{p_1}$. The radiated sound power from the cylinder with respect to the input force is then approximated by:

$$\frac{W}{F^2} = \frac{S}{N}\sum_{n=1}^{N}\frac{I_{R,i}}{F^2}\,, \tag{4}$$

where S is the total external surface area surrounding the cylinder at a distance of 25mm from the surface and N is the number of measurement locations for the sound intensity.

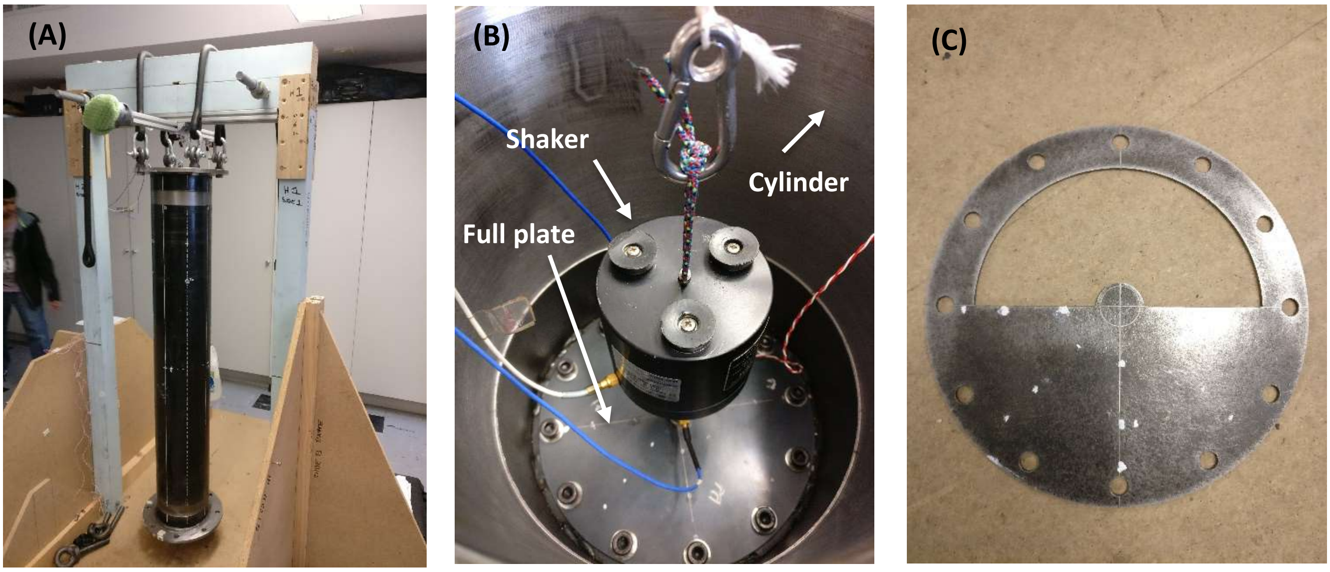

Figure 1: (A) The suspended cylinder, (B) as viewed from above, the assembled full plate with suspended shaker, and (C) the half plate.

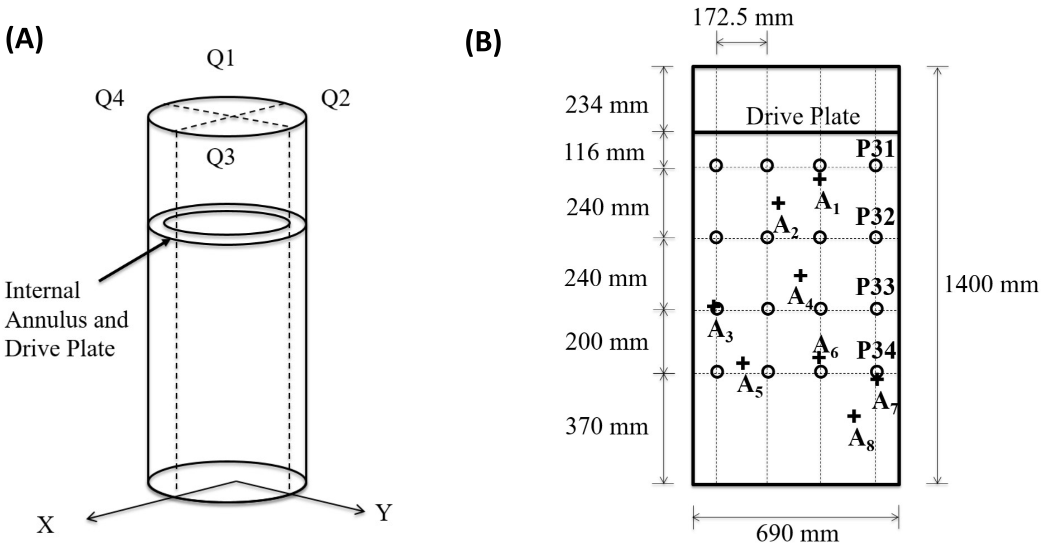

Figure 2: (A) General experimental set-up (B) Overview of measurement locations for sound intensity and acceleration on the cylinder.

3. RESULTS AND DISCUSSION

Figure 3 shows the spatially averaged acceleration with respect to the driving force for the cylinder with the full and half plates measured from the eight accelerometers shown in Figure 2B. The curves in Figure 3 are characterised by resonance peaks and the following observations are made by comparing these curves:

(1) Below 900 Hz, the two curves have five similar resonance frequencies at approximately 331 Hz, 624 Hz, 738 Hz, 777 Hz, and 848 Hz, although the levels at these resonance frequencies can be quite different.
(2) In the frequency range 380–558 Hz, the response of the cylinder with the half plate is high and dominated by several resonant modes, while the response of the cylinder with the full plate is much lower (at least 20 dB lower) than that with the half plate.
(3) In the frequency range 664–859 Hz, the response of the cylinder with the full plate is high and dominated by several resonant modes as well, while the response of the cylinder with the half plate is much lower.
(4) The total numbers of modes found in Figure 3 between 1288 Hz and 1600 Hz for both curves are similar.

The peaks in the two curves have similar resonance frequencies because the vibration at those frequencies is dominated by the cylinder-controlled modes. Although the plate–cylinder coupling may cause some change in the resonance frequencies of the coupled system modes, the coupled resonance frequencies and mode shapes of the cylinder-controlled modes can still be approximated by those of the original cylinder modes (Pan & Hansen, 1991). The increased response level of the cylinder with the half plate at 331 Hz is due to the large mobility function of the half plate at this frequency (see Figure 4). Similarly, the increased response level of the cylinder with the full plate at 777 Hz is due to the large mobility function of the full plate at this frequency. As measured by a laser vibrometer, the distributed vibration of the cylinder with half or full plates at each of these frequencies exhibits similar vibration patterns in the cylinder (see Figure 5).

The cylinder vibration at the resonance frequencies in the half-plate and full-plate dominated regions involves other coupling mechanisms. Taking the responses at 459 Hz (half-plate-controlled mode) and 698 Hz (full-plate-controlled mode) as examples, the driving point mobility shown in Figure 4 clearly indicates that the corresponding resonance peaks are caused by the half-plate-controlled and full-plate-controlled resonances. In these cases, the responses of the cylinder are due to forced vibration, and the measured distribution of the cylinder response is often the superposition of several non-resonant modes of the cylinder. The degree of participation of these non-resonant modes is dependent on the differences between the resonance frequencies of the non-resonant mode and the plate-controlled mode, and the mode shape coupling between the plate and cylinder. Figure 6 shows the measured vibration distributions at these two frequencies and, indeed, it can be seen that they are due to the superposition of several cylinder modes. It is worth noting the small resonance peak at 735 Hz, which is in the vicinity of the full-plate-controlled resonance frequency. This small peak is due to the weakly excited system mode due to the non-resonant excitation of the full plate (see Figure 7). Comparing the distributions at 735 Hz and 698 Hz shows the similarities between them. This is because the modes at the frequencies closest to the full-plate-controlled resonant frequencies generally make the most significant contribution to the forced cylinder responses at these frequencies.

The sound power radiated from the cylinder, calculated from Equation 4, with respect to the input force squared for both the half and full plates is shown in Figure 8. It can be seen that the same features which are present in the average vibration response in Figure 2 are also present here. The half plate exhibits a main peak at 459 Hz and the full plate exhibits a peak at 698 Hz. The bandwidths of these two peaks are also relatively broad. This feature of the sound power demonstrates the effectiveness of sound radiation by the plate-controlled mode of the coupled system and the contribution of the nearby cylinder modes to the bandwidths. It is worth noting that the sound power measured at 698 Hz is approximately equal to that at 459 Hz. This is also seen in the vibration level at 698 Hz and 459 Hz. The first and second resonant peaks of the cylinder are also present in the measured sound power. In addition, it is observed that the greater the average vibration response at a particular frequency, the greater the sound power produced. For example, the average vibration response of the half plate is approximately 20 dB greater than that of the full plate at 331 Hz. This is also observed in the sound power response, where the sound power generated by the half plate at 331 Hz is much greater than the sound power produced by the full plate. This result is expected as sound power is proportional to the mean squared velocity of a given structure.

The sound intensity measurements at each of the sixteen locations are displayed in Figures 9–11. In each graph for the positions defined in Figure 2, the solid and dotted curves are for the cylinder with the full and half plates, respectively. Figure 9 displays the sound intensity recorded between 300 and 400 Hz, where the first cylinder mode due to the half-plate excitation dominates. Thus, in this frequency range, the measured sound intensities from the cylinder with the half plate are much larger than that from the cylinder with the full plate. Figure 10 displays the sound intensity recorded between 400 and 500 Hz, where the half-plate-controlled mode dominates the cylinder vibration. In this case, a large positive sound intensity is observed in the bottom and top parts of the cylinder, and some small negative sound intensity is observed in the middle of the cylinder, indicating that some sound energy actually flows back to the cylinder. Figure 11 displays the sound intensity recorded between 600 and 750 Hz, where the full-plate-controlled mode dominates the vibration at 698 Hz and the vibration response of the cylinder with the half and full plates lies at a similar level at 624 Hz. Indeed, near the later frequency, comparable sound intensity levels can be acquired from the cylinder with both half and full plates. The slight shift of peak frequencies between the two cases can be traced back to the shift of peak frequencies in the vibration response shown in Figure 3. The distribution of sound intensity from the cylinder with the full plate around 698 Hz is characterized by relative large amplitudes and frequency band peaks. This is explained by the similar features in the cylinder vibration response.

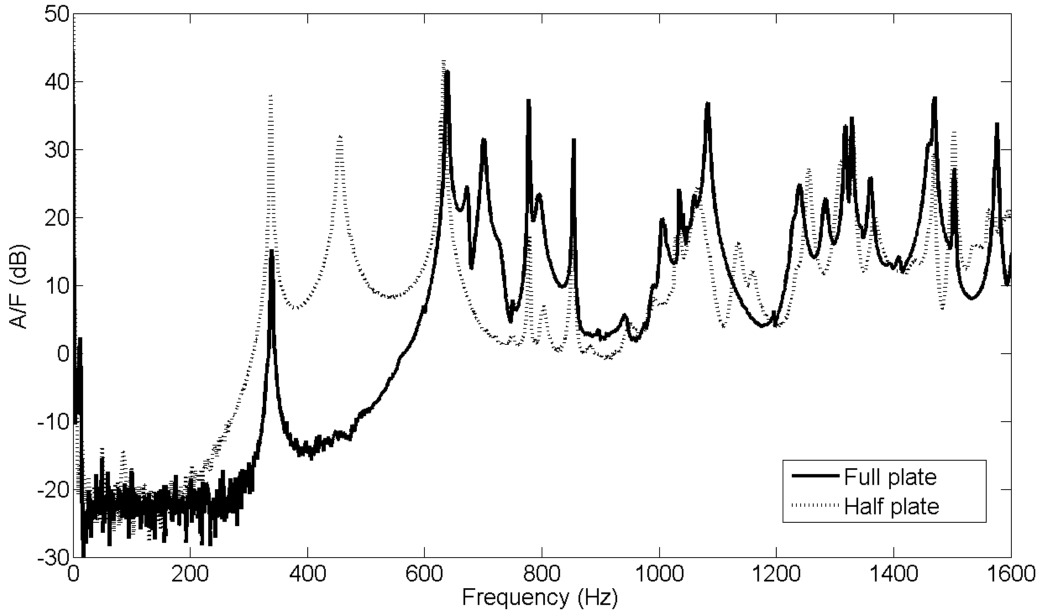

Figure 3: Spatially averaged acceleration with respect to the driving force for the cylinder with the full and half plates.

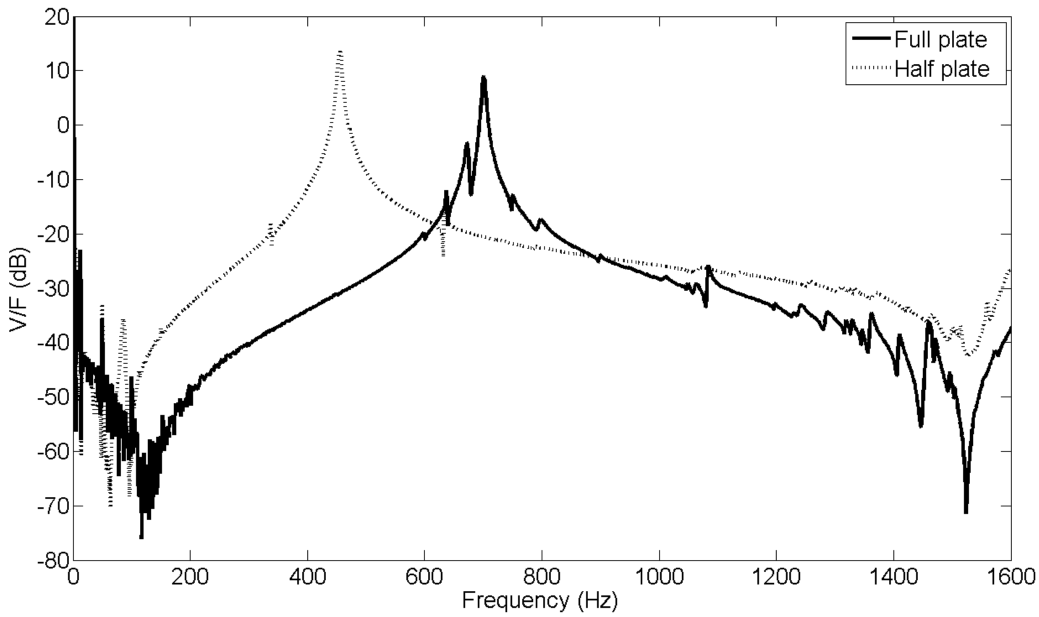

Figure 4: Input mobility for the cylinder with the full and half plates.

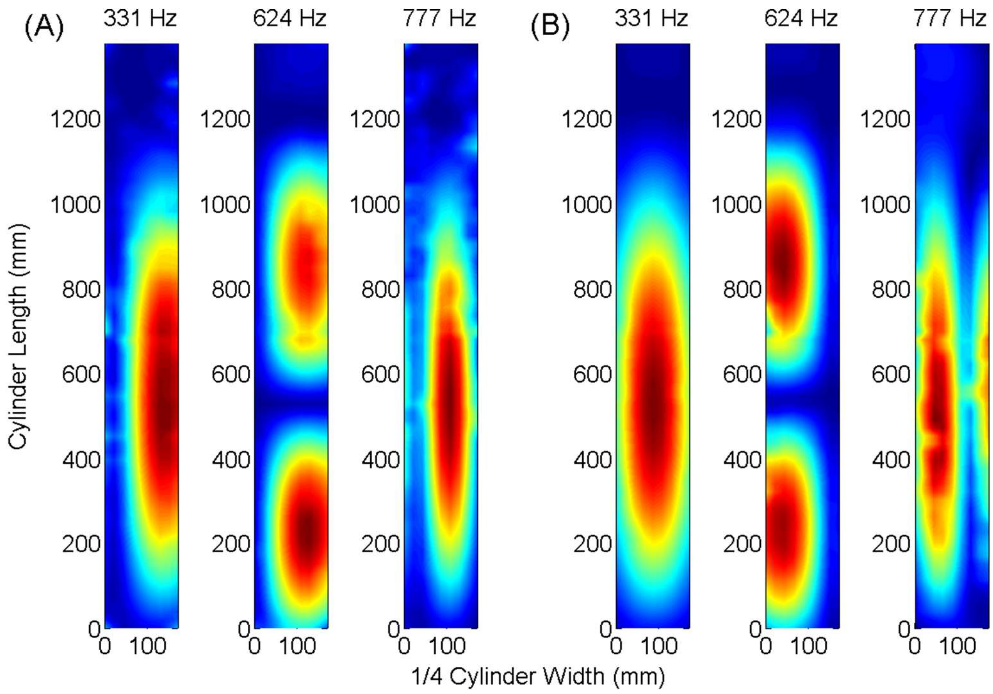

Figure 5: One-quarter of cylinder surface vibration from laser vibrometer measurements for (A) Full-plate and (B) half-plate mode shapes at 331, 624, and 777 Hz. Note that each plot has a different scale, which has been omitted for clarity.

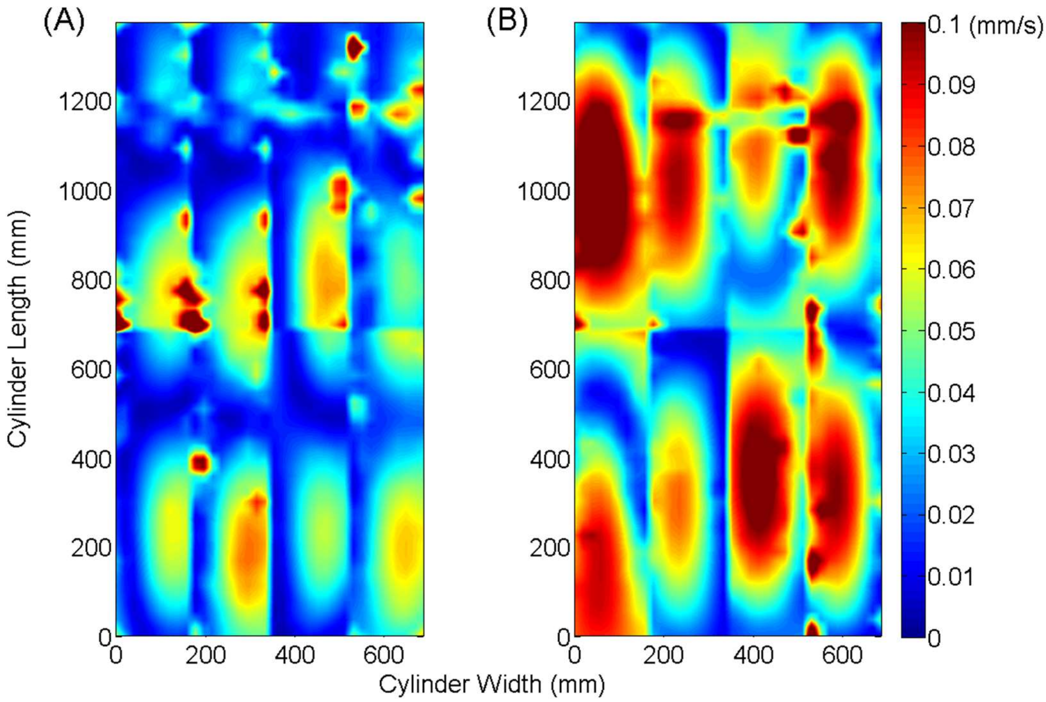

Figure 6: Cylinder surface vibration from laser vibrometer measurements for (A) Full-plate response at 698 Hz and (B) half-plate response at 459 Hz.

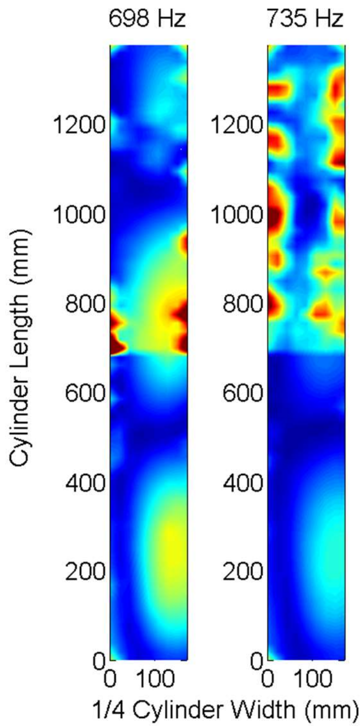

Figure 7: One-quarter of cylinder surface vibration from laser vibrometer measurements for full plate at 698 Hz and 735 Hz.

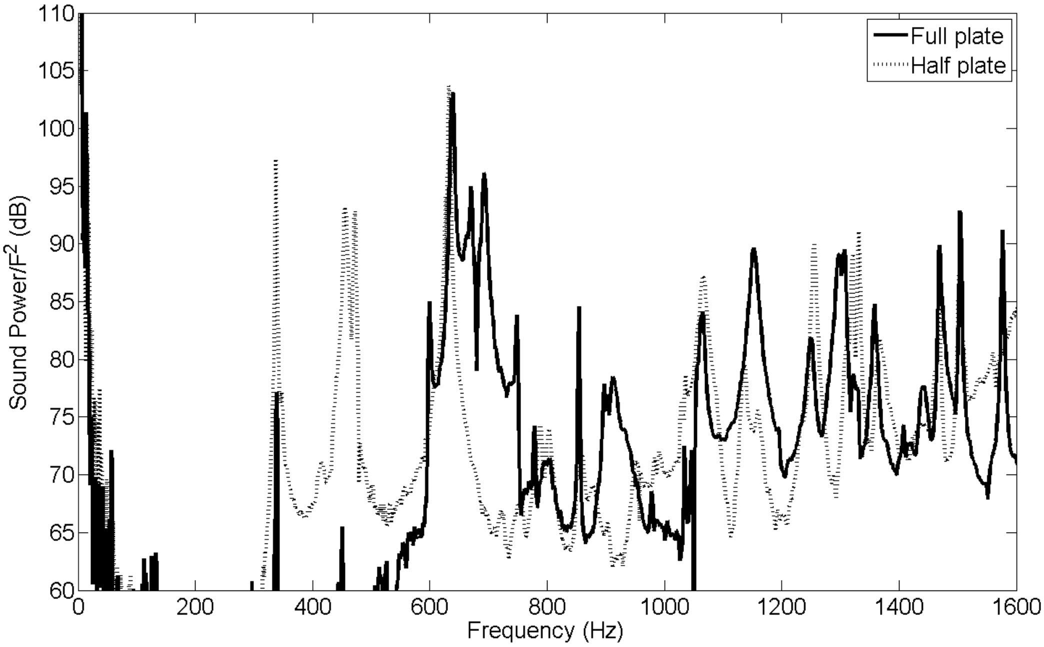

Figure 8: Total sound power for the cylinder with the full and half plates, with respect to the input force squared.

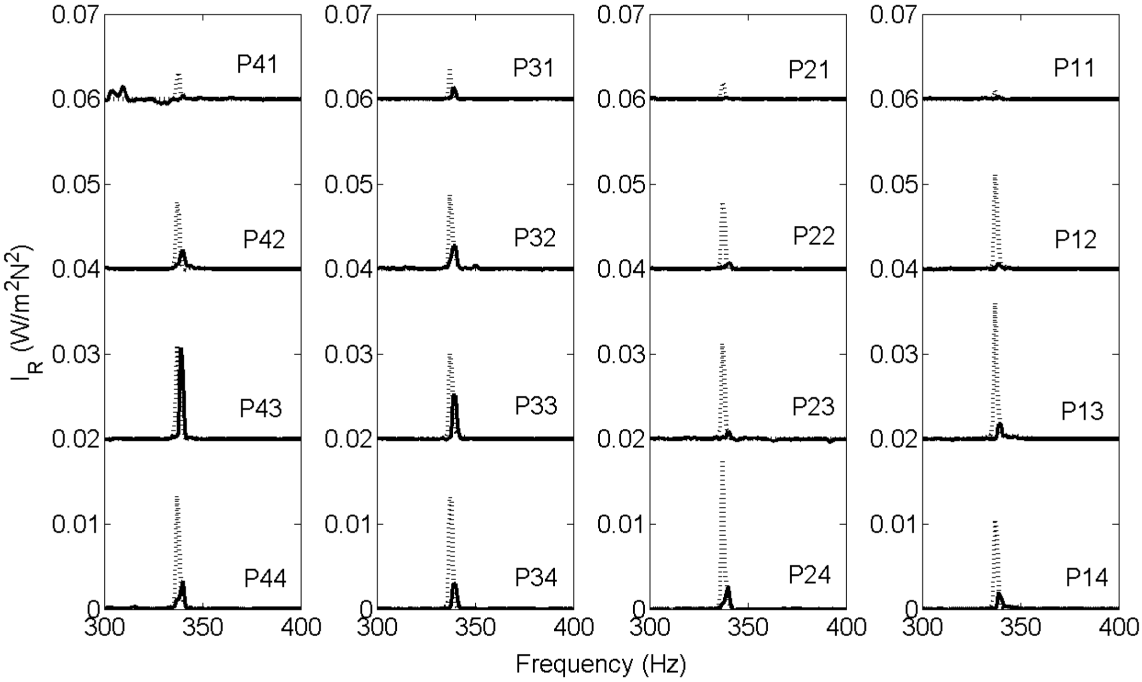

Figure 9: Sound intensity with respect to the input force squared between 300 and 400 Hz. Each curve is offset by 0.02 from the one underneath for clarity. Full plate results increased by a factor of 100 for clarity. Full plate —— half plate ······.

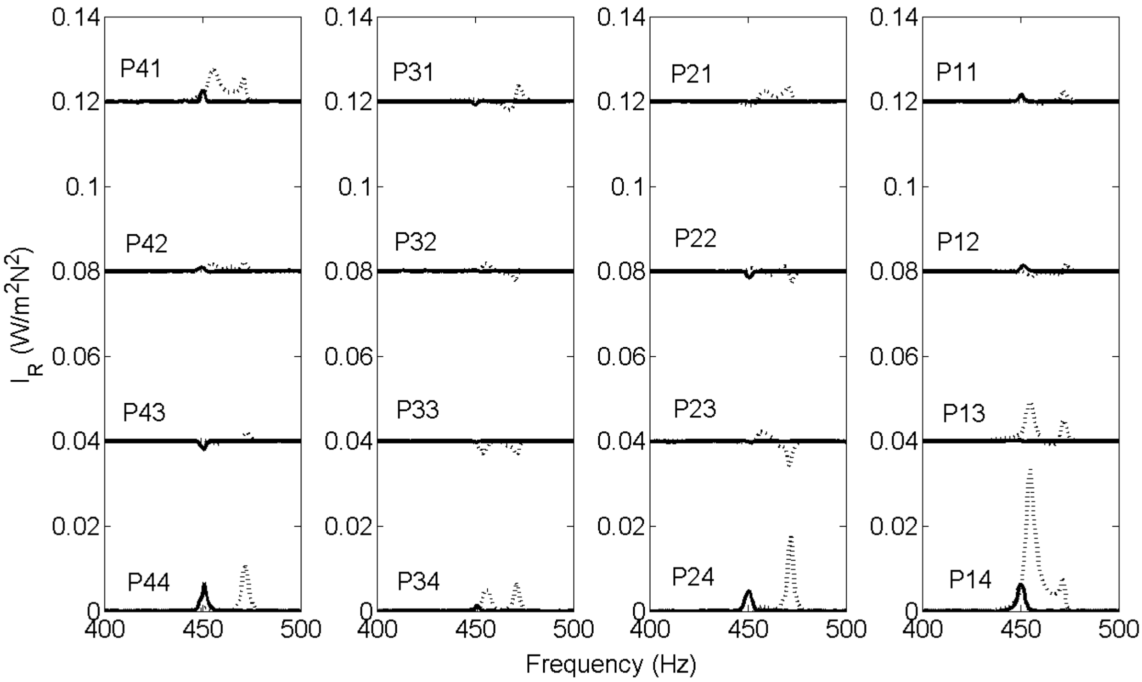

Figure 9: Sound intensity with respect to the input force squared between 400 and 500 Hz. Each curve is offset by 0.02 from the one underneath for clarity. Full plate results increased by a factor of 100 for clarity. Full plate —— half plate ······.

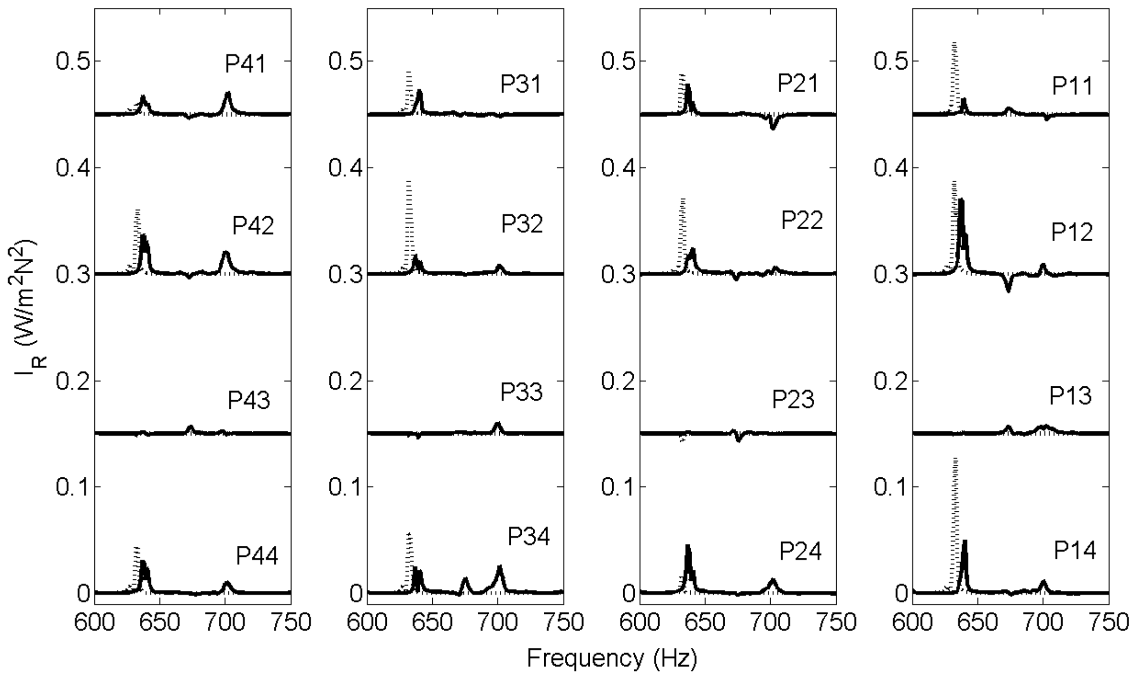

Figure 11: Sound intensity with respect to the input force squared between 600 and 750 Hz. Each curve is offset by 0.6 from the one underneath for clarity. Full plate —— half plate ········.

4. CONCLUSION

This paper provided experimental evidence to illustrate that the coupling between the thrust-bearing bulkhead and hull structure may have a significant effect on the sound radiation of the hull of a marine vessel. The experiment was implemented on a coupled plate–cylinder structure. A force-driven half plate and full plate were used to examine the effects of the different modal characteristics of a "thrust-bearing" plate on the cylinder vibration and sound radiation.

It has been observed that, at the resonance of the plate-controlled mode, the cylinder has the potential to radiate large sound power. In this case, an effective reduction of sound radiation can be realized by reducing the resonance response of the thrust-bearing plate and controlling the coupling between the plate and cylinder.

The cylinder also has the potential to radiate sound in the cylinder-controlled modes. In this case, the magnitude of sound radiation is also determined by how close the resonance frequencies of the cylinder-controlled modes are from the resonance frequencies of the thrust-bearing plate.

Further work in this direction of research includes optimal structural design of the thrust-bearing plate for minimum sound radiation from the cylinder at the major disturbance frequencies of the thrust. The effect of coupling between the radiation environment and the cylinder and between the thrust-bearing plate and the cylinder on the sound radiation will also be included in future work.

REFERENCES

Caresta, M & Kessissoglou, N 2009, 'Structural and acoustic responses of a fluid-loaded cylindrical hull with structural discontinuities', *Journal of Applied Acoustics,* vol. 70 no. 1 pp. 954-963.

Caresta, M & Kessissoglou, N 2010, 'Acoustic signature of a submarine hull under harmonic excitation', *Applied Acoustics,* vol. 71 no. 1 pp. 17-31.

Fahy, F 1987, *Sound and Structural Vibration.* Academic Press, London.

Gangemi, PJ & Kanapathipillai, S 2014, 'Submarine structural and acoustic attenuation', *Journal of Vibration and Control,* vol. 22 no. 14 pp. 3135-3150.

Leader, J, Pan, J, Dylejko, P & Matthews, D 2013, 'Experimental investigation into sound and vibration of a torpedo-shaped structure under axial force excitation', *The Journal of the Acoustical Society of America,* vol. 133 no. 5 pp. 3517-3517.

Leissa, AW 1973, *Vibration of Shells,* National Aeronautics and Space Administration, Washington D.C.

Merz, S, Oberst, S, Dylejko, P, Kessissoglou, N, Tso, YK & Marburg, S 2006, 'Development of coupled FE/BE models to investigate the structural and acoustic responses of a submerged vessel', *Journal of Computational Acoustics,* vol. 15 no. 1 pp. 23-47.

Merz, S, Kinns, R & Kessissoglou, N 2009, 'Structural and acoustic responses of a submarine hull due to propeller forces', *Journal of Sound and Vibration,* vol. 325 no. 1 pp. 266-286.

Pan, J & Hansen, CH 1991, 'Active control of noise transmission through a panel into a cavity. II: Experimental study', *Journal of the Acoustical Society of America,* vol. 90 no. 3 pp. 1488-1492.

Soedel, W 2004, *Vibrations of Shells and Plates,* Marcel Dekker, New York.

Tyack, P 2008, 'How sound from human activities affects marine mammals', *The Journal of the Acoustical Society of America,* vol. 123 no. 5 pp. 2969-2969.